U.S. Department of Energy, Office of Science
Environmental Remediation Sciences Division (ERSD)
FY08 Third Quarter Performance Measure

Introduction

This report is the third in a series of quarterly progress reports from the Rifle IFC project on the ERSD general performance measure: **"Identify the critical redox reactions and metabolic pathways involved in the transformation/sequestration of at least one key DOE contaminant in a field environment."** The first quarter report documented the approach to identify critical redox reactions in the subsurface during stimulated uranium biotransformation. The second quarter report documented the approach to identify key microbial metabolic processes in the subsurface during stimulated uranium biotransformation. The topic of this report (Third Quarter Performance Measure) is the development of the conceptual process models from the new uranium biotransformation knowledge and the approach to coupling these models in numerical simulations of field scale flow and reactive transport.

Background

In 2002, a series of uranium bioremediation field experiments began at the Old Rifle Uranium Mill Tailings Remedial Action (UMTRA) site in Western Colorado (subsequently referred to as the Rifle IFC site). The principle of direct enzymatic reduction of mobile hexavalent uranium [U(VI)] that these field experiments were based on was identified more than 10 years earlier by Lovley et al. (Lovley et al. 1991) and Gorby and Lovley (Gorby and Lovley 1992) who suggested that dissimilatory metal-reducing bacteria grown on acetate could be used to immobilize U(VI) as precipitated U(IV) mineral. In particular, the 2002 and 2003 biostimulation field experiments, which were performed in the same field plot (**Figure 1**) at the Rifle IFC site (Anderson et al. 2003; Vrionis et al. 2005), demonstrated that U(VI) concentrations in the shallow unconfined aquifer could be lowered below relevant standards by stimulating indigenous dissimilatory metal reducing bacteria with acetate as the electron donor. The removal of U(VI) from solution was coincident with a decrease in Fe(III) minerals, an accumulation of Fe(II) and an enrichment of *Geobacteraceae*, which led to the attribution of uranium bioreduction to iron-reducing *Geobacter* species. The greatest enrichment of *Geobacteraceae* in sediments was correlated to the highest ratio of U(IV) to total uranium. This was followed by a sulfate-reducing phase characterized by the simultaneous observance of sulfide, depleted Fe(III), and 16S rDNA sequences most closely related to *Desulfobacterales*. The transition to sulfate-reducing conditions, as evidenced by a decrease in sulfate concentrations after 45 days of acetate amendment in 2002, was accompanied by a decrease in U(VI) removal efficiency from the groundwater (Anderson et al. 2003). The field observations, including downgradient sediment cores with elevated U(IV), were consistent with previous laboratory studies where 1) the stimulation of acetate-oxidizing metal reducing bacteria (i.e., *Geobacter sp.*) concomitantly reduced and immobilized aqueous U(VI)[(Finneran et al. 2002; Holmes et al. 2002)], and 2) acetate-oxidizing sulfate reducing bacteria were not as effective at

U(VI) immobilization(Lovley et al. 1993; Ortiz-Bernad et al. 2004)

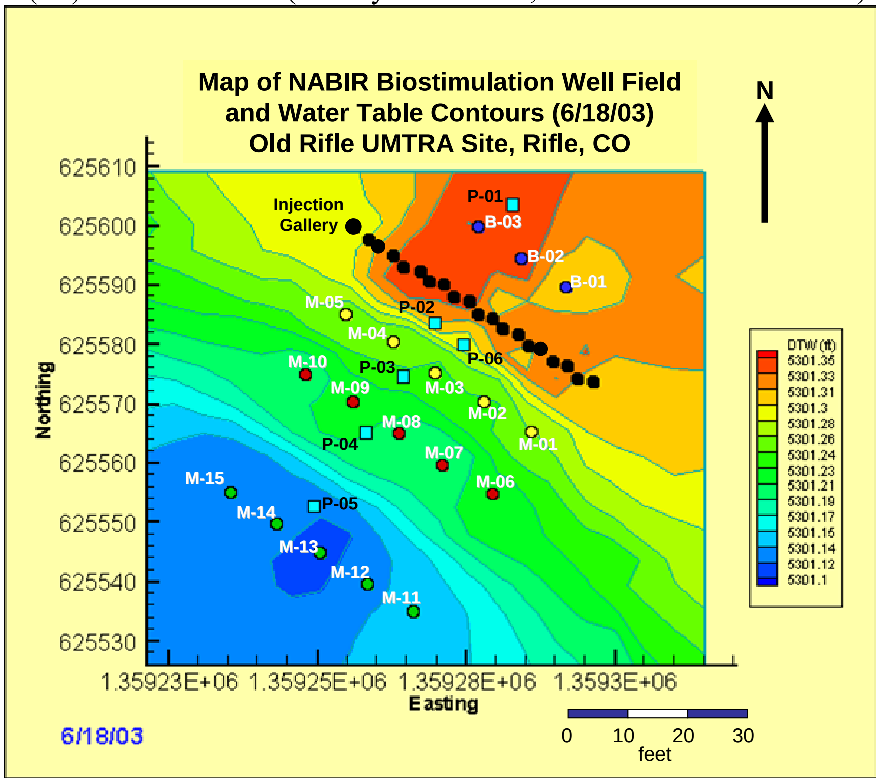

Figure 1. Well layout and potential surface. Numbered downgradient monitoring wells are denoted with the prefix M, numbered upgradient monitoring wells are denoted with the prefix B, and numbered sediment sampling coreholes are denoted with the prefix P.

Previous Reactive Transport Modeling. A reactive transport modeling study by Yabusaki et al. (2007) analyzed data from the 2002 and 2003 field experiments, and characterized the principal flow, transport and biological processes controlling uranium mobility during the experiments. Data from the 2002 field experiment were used to identify the dominant transport and biological processes controlling uranium mobility during biostimulation, and determine field-scale parameters for these modeled processes. Under the very low dissolved oxygen and nitrate conditions in the Rifle IFC groundwater, the biostimulation was assumed to quickly proceed to iron reduction with negligible consumption of electron donor by the oxygen and nitrate TEAPs. Microbial community composition and function from (Anderson et al. 2003) provided insight on the differentiation of the metabolic capability associated with specific community members related to uranium immobilization. A simple process model conceptualization with three terminal electron acceptor processes (TEAPs) with two distinct immobile microbial populations was chosen to build an understanding of the dominant behaviors of the bulk system observed in the field at the Rifle IFC site.

$$0.125\ CH_3COO^- + 0.6\ FeOOH(s) + 1.155\ H^+ + 0.02\ NH_4^+ = 0.02\ BM\_iron + 0.6\ Fe^{++} + 0.96\ H_2O + 0.15\ HCO_3^- \quad (1)$$

$$0.125\ CH_3COO^- + 0.3875\ UO_2^{++} + 0.3538\ H_2O + 0.0113\ NH_4^+ = 0.0113\ BM\_iron + 0.3875\ UO_2(s) + 0.855\ H^+ + 0.1938\ HCO_3^- \quad (2)$$

0.125 CH_3COO^- + *0.1155* SO_4^{--} + *0.0057* H^+ + *0.0038* NH_4^+ = *0.0038 BM_sulfate* + *0.1155* HS^- + *0.114* H_2O + *0.231* HCO_3^- (3)

Acetate injection initially stimulates the growth of *Geobacteraceae*, resulting in the reduction of Fe(III) as well as the removal of U(VI) from groundwater (**Equation 1 and 2**). The second phase of the conceptual model of biologically-mediated reactions is sulfate-reduction, triggered presumably by the depletion of a threshold amount of bioavailable Fe(III). In this case, the TEAP reaction for sulfate reduction is associated with immobile sulfate-reducing organisms (BM_sulfate in **Equation 3**).

The stoichiometry in these irreversible reactions, which include the yield of an immobile biomass, are energetics-based (Rittmann and McCarty 2001) under the assumption of a biomass molecular formula of $C_5H_7O_2N$ and an energy-transfer efficiency value of 0.6. In these three TEAP reactions, the biomass is nominally attributed to iron-reducing organisms (BM_iron in **Equations 1 and 2**) that are known to be dominated by *Geobacter* sp. Goethite, one of the iron oxides identified by Mössbauer spectroscopy (Komlos et al. 2008) was used as an Fe(III) oxide terminal electron acceptor. Uranyl is used as terminal electron acceptor in the uranium reduction reaction (**Equation 2**). The ammonium ion, NH_4^+ is considered to be non-limiting.

The kinetics of the microbially-mediated redox reactions is of Monod-type augmented by a thermodynamic control term for all the TEAP reactions. The rate law in **Equation 4** is used in conjunction with the three biogeochemical reactions to determine the acetate consumption rate, R_C^{bio},

$$R_C^{bio} = -\sum_{eA}^{N_{eA}} \chi_{eA}\mu_{m,eA}\left(\frac{C_C}{K_{s,C}+C_C}\right)\left(\frac{C_{eA}}{K_{s,eA}+C_{eA}}\right)f(\Delta G_r) \tag{4}$$

where N_{eA} is the number of terminal electron acceptors, C_c is acetate concentration, C_{eA} is the terminal electron acceptor concentration, $\mu_{m,eA}$ is the acetate oxidation rate for the terminal electron acceptor, $K_{s,C}$ is the half-saturation coefficient for acetate, $K_{s,eA}$ is the half-saturation coefficient for the terminal electron acceptor, and $f(\Delta G_r) = 1 - \exp[(\Delta G_r - \Delta G_{min})/RT]$ (ΔG_r is the free energy of the corresponding TEAP reaction, ΔG_{min} is the minimum energy required to drive ATP synthesis, R is the gas constant, T is the absolute temperature). χ_{ea} is the indicator coefficient for terminal electron acceptor utilization which is not related to thermodynamics and is determined by the concentration of the precedent terminal electron acceptor which is more energetically favorable.
χ_{ea} is equal to 1 when the electron acceptor in the redox reaction is being utilized and equal to 0 when a redox reaction involving a more energetically favorable electron acceptor still dominates. In other words, the utilization of a less favorable terminal electron acceptor does not proceed until the concentration of the more favorable electron acceptor drops below a specified threshold level (Kindred and Celia 1989; Kinzelbach et al. 1991; Rabouille and Gaillard 1991; Park and Jaffe 1996). Introduction of χ_{ea} was based on the onset of sulfate reduction after the consumption of a threshold amount of bioavailable Fe(III) mineral.

In the case of iron oxide reduction, the second Monod term is replaced by the Fe(III) mineral in equivalent molarity. The rates and threshold concentration for utilization of the terminal electron acceptors were calibrated using the 2002 field experiment observations of acetate, Fe(II), U(VI), and sulfate.

The coupled process simulation approach was able to establish a quantitative characterization of the principal flow, transport, and reaction processes based on the 2002 field experiment, that could be applied without modification to describe the 2003 field experiment. In **Figures 2 to 4,** simulation results based on the 2002 calibrated data set are compared with observed breakthrough curves for acetate, sulfate, and uranium, respectively. Acetate is assumed to be initially consumed by iron-reducers that also utilize U(VI) as a terminal electron acceptor. Using the initial ratio of bromide to acetate before release from the injection gallery, acetate consumption during the iron reduction phase was estimated to be ca. 35%, 45%, and 85% to the first, second and third rows of monitoring wells, respectively.

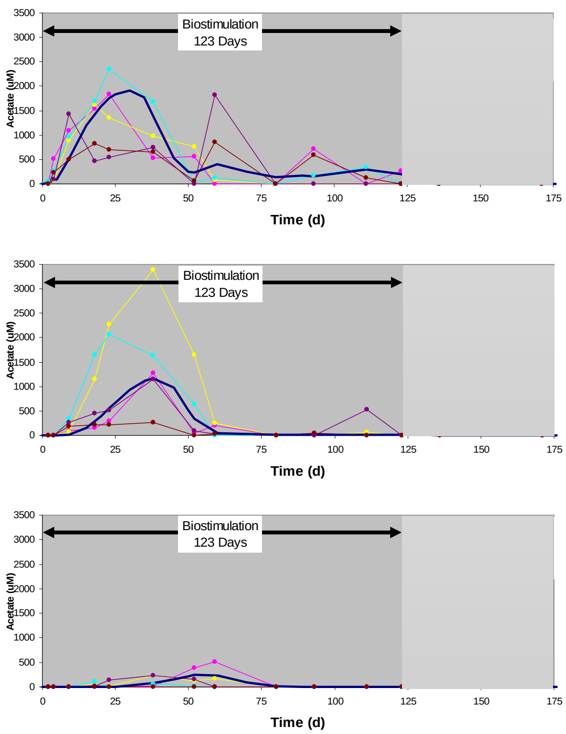

Figure 2. 2002 field experiment: simulated (dark blue line) and observed (colored lines/symbols) acetate breakthrough for monitoring wells 3.7 m (top), 7.3 m (center), and 14.6 m (bottom) downgradient from injection gallery.

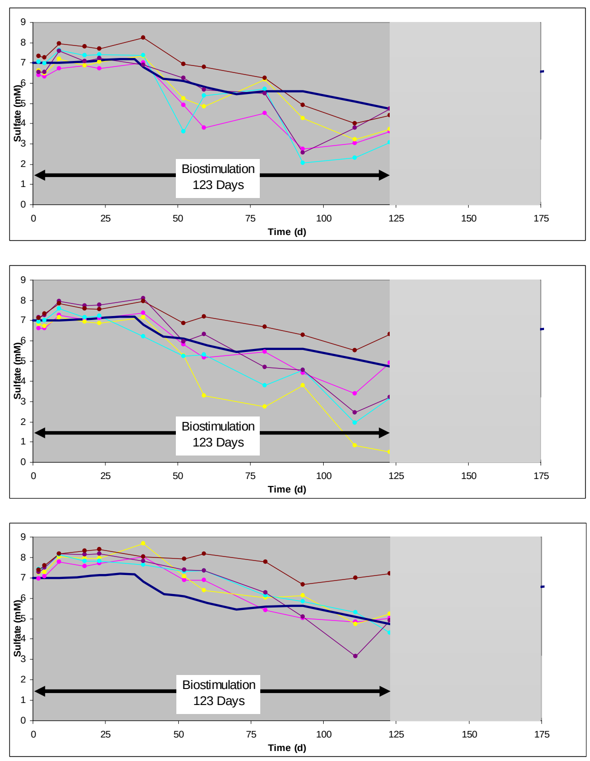

Figure 3. 2002 field experiment: simulated (dark blue line) and observed (colored lines/symbols) sulfate breakthrough for monitoring wells 3.7 m (top), 7.3 m (center), and 14.6 m (bottom) downgradient from injection gallery.

It should be noted that the observed increase in aqueous Fe(II) concentrations (ca. 80 μM), while a qualitative indicator of Fe(III) bioreduction, is a small fraction of the Fe(II) generated by the simulated iron TEAP (ca. 5 mM in the first row of monitoring wells). Therefore the bulk of the Fe(II) generated by the iron-reducers is assumed to be associated with the solid phases.

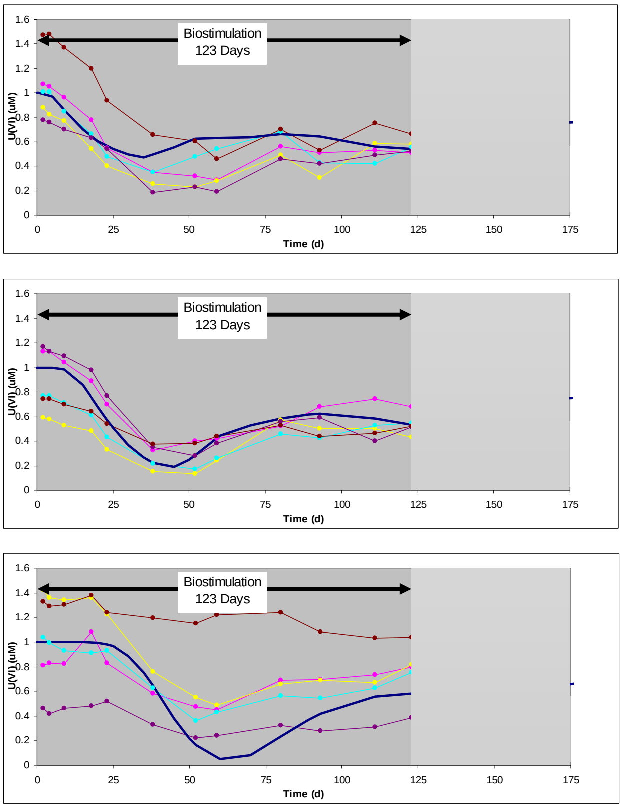

Figure 4. 2002 field experiment: simulated (dark blue line) and observed (colored lines/symbols) U(VI) breakthrough for monitoring wells 3.7 m (top), 7.3 m (center), and 14.6 m (bottom) downgradient from injection gallery.

Although acetate was released from the injection gallery for 123 days, acetate concentrations began to decline after 40, 50, and 60 days in monitoring rows 1, 2, and 3 respectively, followed by depletion in most of the wells after 50, 60, and 80 days, respectively (**Figure 2**). The decline of acetate concentrations coincided with the onset of sulfate reduction as evidenced by the concomitant decrease in sulfate concentrations (**Figure 3**). The eventual depletion of acetate occurs because of several factors: 1) in the postulated reaction stoichiometry, one mole of acetate reacts with 0.924 moles of sulfate [versus 4.8 moles of Fe(III) and 6.2 moles of U(VI) in the iron and uranium TEAPs, respectively], 2) sulfate concentrations are approximately three times the initial acetate concentrations in the groundwater, and 3) the sulfate bioreduction rate is relatively rapid. This results in an acetate-limited sulfate bioreduction reaction that continues to completely consume acetate to the end of the biostimulation period. These general descriptions are tempered by the spatial and temporal variability of the bromide and acetate breakthrough curves: multiple peaks with later arrivals in Row 1 and the highest concentrations being observed in Row 2 rather than Row 1. While there is evidence in the drilling logs for heterogeneities in the aquifer sediments (Vrionis et al. 2005), the observed spatial and temporal variability in the tracer behavior is also due, in part, to variability in the injection rate of the amendment solution to individual wells in the injection gallery.

The bioreduction and immobilization of U(VI) in groundwater is clearly most efficient in the presence of the iron reducers, so the maintenance of this condition is a desirable bioremediation goal. In the current conceptual model, the consumption of a threshold amount of bioavailable Fe(III) mineral near the point of acetate injection leads to the onset of sulfate reduction, which has significant implications at the Rifle IFC site because of the high sulfate concentrations (ca. 8 mM) in the groundwater. In the 2002 field experiment, the local depletion of bioavailable iron resulted in the onset of sulfate reduction that consumed nearly all of the influent acetate, preventing the further enrichment of downgradient iron-reducers capable of uranium bioreduction. Thus, one important outcome of the modeling was a field estimate of the bioavailable Fe(III) mineral threshold for sulfate reduction at 0.88 μmol g^{-1} of bulk sediment. This is a relatively small fraction of the extractable Fe(III) [2 h 0.5 N HCl extraction with hydroxylamine] in the background sediments, which ranged from 2.4 to 21 μmol g^{-1} in the background borehole P-01 after assuming that the > 2 mm size fractions (73% by weight) were inert. In addition, this interpreted field value is slightly less than half of the 1.9 μmol g^{-1} laboratory estimate of poorly crystalline iron in background sediments from the Rifle IFC site, using a 1-hour iron extraction in 0.5 N HCl with 0.25 N hydroxylamine and employing a similar correction for the whole sediment.

Vrionis et al. (2005) provided geochemical evidence suggesting that Fe(III), U(VI), and sulfate reduction could simultaneously occur during acetate biostimulation in the field. This observation was bolstered by the presence of both *Geobacteraceae* and *Desulfobacterales* in the associated sediment sample. Accordingly, a rate law was developed for the Fe(III) TEAP that allowed iron reducer activity to continue after the onset of the sulfate reducers. In this case, the lower rate of U(VI) removal from groundwater observed during sulfate reduction was attributed to the lower activity of iron reducers competing with sulfate reducers for the electron donor, acetate. Thus, the estimate of the bioavailable Fe(III) threshold for the onset of sulfate reduction is not an intrinsic limit on the Fe(III) mineral that can be utilized as a terminal electron acceptor. In systems where acetate is not limiting, it is possible that the iron reducers would be able to utilize significantly more Fe(III) after the onset of sulfate reduction, albeit less efficiently. This behavior is consistent with observations of low sulfate column experiments performed with sediments from the Rifle IFC site (Moon et al. 2007).

Incorporation of Abiotic Reaction Processes

The Rifle biostimulation modeling study by Yabusaki et al. (2007) resulted in field-scale estimates of the bioavailable Fe(III) mineral threshold for the onset of sulfate reduction, and rates for the Fe(III), U(VI), and sulfate terminal electron accepting processes. The focus on microbially-mediated TEAPs allowed early progress under a simple conceptualization of the reaction network. Clearly, a combination of hydrologic, geochemical, and biological factors control the effectiveness of the uranium immobilization, making it a challenge to reliably predict important behaviors during and after bioremediation. An important consideration is the impact of changes in the geochemical environment induced by the biostimulation with acetate amendment. Of interest is the abiotic response (e.g., mineral precipitation and dissolution, aqueous and surface complexation) to the reduced oxidation state species U(IV), Fe(II) and sulfide produced during the experiments as well as the lowered redox potential. These reactions, strongly associated with the solid phases, may play an important role in stabilizing long-term uranium immobilization. The inclusion of abiotic chemistry in the modeled reaction network is also necessary to account for changes in solution chemistry (e.g., pH, alkalinity, and calcium) that nominally control uranium speciation and mobility. Uranium has a broad range of mobility that is dependent on the redox state of the dissolved uranium, ambient water chemistry, and the surface reactivity of the subsurface sediments (Davis and Kent 1990; Curtis et al. 2004; Davis et al. 2004; Davis et al. 2006b).

The current conceptual model for uranium behavior at the Rifle IFC site (Anderson et al. 2003; Chang et al. 2005; Vrionis et al. 2005) has the bulk of uranium in the aquifer originating as leachate from mill tailings (now removed), percolating through a 4 m thick vadose zone to the water table, and transported laterally through the aquifer via groundwater flow. Groundwater moves primarily in the topmost hydrostratigraphic unit of the unconfined aquifer, a sandy-gravel, gravelly-sand alluvium with an average saturated thickness of 2.4 meters in the vicinity of the experimental plot. This permeable layer (hydraulic conductivity ca. 35 md^{-1}) is underlain by a relatively impermeable silty shale (conductivity ca. 0.005 md^{-1}) from the weathered Wasatch formation (DOE 1999).

Based on analyses of groundwater samples during 2002, 2003 and 2007, the aquifer is characterized by very low dissolved oxygen (<0.2 ppm), although higher measurements are observed near the water table and during elevated water table conditions in late spring. Nitrate concentration is commonly below detection. The low nitrate concentrations are consistent with the presence of Fe(II) (ca. 50 uM) in solution and an Eh of ca. 150 mV at circumneutral pH. Background aqueous sulfate concentrations range from 6 to 11 mM.

Uranium Surface Complexation. The uranium migrates through the subsurface as hexavalent U(VI), exceeding the applicable regulatory standard of 44 μgL^{-1} (EPA 1998) throughout the experimental site, with maximum concentrations ca. 300 μgL^{-1}. Surface complexation is an important process in attenuating the mobility of uranium in the subsurface environment (Pabalan et al. 1996; Moyes et al. 2000). Under the ambient pH and alkalinity at the Rifle IFC site, a significant fraction of the U(VI) (principally as uranyl and uranyl carbonate) would be expected to adsorb to the sediments via surface complexation. Brooks et al. (2003) provided experimental evidence of the strong influence of calcium on the sorption of U(VI), through competition of the aqueous complex $Ca_2UO_2(CO_3)_3$ with the iron surface complexes.

Laboratory characterizations were performed to develop a quantitative understanding of uranium adsorption in this study. We used the generalized composite surface complexation modeling approach developed by Davis et al. (2004) to model uranium sorption. In this non-electrostatic model, 2 sorption reactions occurring at 3 different sites were used: very strong sites (>SSOH), strong sites (>SOH) and weak sites (>WOH) defined by their relative binding strength for U(VI), assuming a total site density of 3.84 umoles/m^2 of hydroxyl groups. The modeled reaction network uses 23 aqueous uranium complexation reactions (including Ca-UO_2-CO_3 ternary complexes). When uranyl is being depleted from the groundwater, the aqueous U(VI) complexes will correspondingly diminish under the equilibrium assumption for these uranium complexation reactions. Stability constants for the 6 surface complexation reactions in **Table 1** were parameterized using BIOGEOCHEM (Fang et al. 2003; Fang et al. 2006) and PEST (Doherty 2004).

Table 1. Uranium surface complexation reactions and stability constants.	
Surface species	
Reaction	logK
$SSOH + UO_2^{2+} = SSOUO_2^+ + H^+$	12.28
$SOH + UO_2^{2+} = SOUO_2^+ + H^+$	6.95
$WOH + UO_2^{2+} = WOUO_2^+ + H^+$	2.74
$SSOH + UO_2^{2+} + H_2O = SSOUOOH + 2H^+$	0.033
$SOH + UO_2^{2+} + H_2O = SOUOOH + 2H^+$	-2.12
$WOH + UO_2^{2+} + H_2O = WOUOOH + 2H^+$	-5.01
SSOH denoting very strong binding sites: 0.01% of total sites SOH denoting strong binding sites: 0.1% of total sites WHO denoting weak binding sites: 99.89% of total sites	

Phyllosilicate Iron Reduction. The preferential bioreduction of phyllosilicate Fe(III) over Fe-oxides was recently identified in Rifle IFC laboratory studies by Komlos et al. (2008) permitting an important refinement to the conceptual model of processes and properties controlling uranium mobility during biostimulation with acetate amendment. Phyllosilicate iron bioreduction accounted for ~90% of the bioreduced iron, with the remainder attributed to the reduction of iron oxides and oxyhydroxides. In this case, the biogenic ferrous iron tends to remain in the layer silicate structure as opposed to the reductive dissolution of the Fe(III) oxides. Accordingly, the reactive transport model now accounts for parallel bioreduction of iron oxides and an additional sediment iron TEAP associated with phyllosilicate (**Equation 5**). Phyllosilicate iron bioreduction is faster and accounts for ~90% bioreduced iron. In this case, the bioavailable iron threshold for the onset of sulfate reduction is now linked to the phyllosilicate iron.

$$0.125\ CH_3COO^- + 0.903\ Fe(III)(ls) + 0.437\ H_2O + 0.00485\ NH_4^+ = 0.00485\ BM\_iron + 0.226\ HCO_3^- + 0.813\ Fe(II)(ls) + 0.09\ Fe^{++} + 1.01H^+ \quad (5)$$

Mineral Reactions. Based on the background chemical conditions, calcite, siderite and iron sulfide were added in the above reaction network and their reaction rate formulations as a function of the saturation state follow (Hunter et al. 1998):

$$R_i = \begin{cases} k_i\left(\Omega_i - 1\right) & \text{for } \Omega_i \geq 1 \\ k_{-i}\left[Q_i\right]\left(\Omega_i - 1\right) & \text{for } \Omega_i < 1 \end{cases} \quad (6)$$

where i represents the i-th mineral phase, R_i is the rate of the reaction, k_i is the mineral precipitation rate [$ML^{-3}T^{-1}$], k_{-i} is the mineral dissolution rate [$ML^{-3}T^{-1}$], Q_i is the concentration of the i-th mineral phase [ML^{-3}], and Ω_i is the saturation index of the i-th mineral phase.

Thermodynamically, it is favorable for magnetite and ferrihydrite, to react with HS^- generated from sulfate reduction to produce Fe(II). Magnetite was identified by Komlos et al. (2008) as a component in the Rifle sediment mineral assemblage. Consequently, we used magnetite as the nominal iron mineral for this reaction.

$$4Fe_3O_4(s) + HS^- + 11\ H_2O = 12Fe^{2+} + SO_4^{2-} + 23OH^- \quad (7)$$

Numerical Simulation Approach**.** The HYDROGEOCHEM simulator (Yeh et al. 2004) provides the framework for incorporating and coupling the flow and reactive transport process models in this investigation. In particular, the multicomponent biogeochemical reaction solver technology (Fang et al. 2003; Fang et al. 2006) addresses mixed kinetic and equilibrium reactions that describe aqueous and surface complexation, oxidation-reduction, mineral precipitation and dissolution, and the microbially-mediated transformations. A systematic approach was taken to model the biostimulation experiments. A reaction network involving background species Ca^{2+}, Mg^{2+}, Na^{+}, Fe^{2+}, H^{+}, CO_3^{2-}, Cl^{-}, SO_4^{2-} , and acetate was first identified, with reaction stoichiometry and thermodynamics at 20°C obtained from the EQ3/6 thermodynamic database (Wolery 1992).

Application to Rifle IFC Field Experiments

A new field experiment plot was employed at the Rifle IFC site in the summer of 2007, about 35 m southeast from the 2002/2003 field plot. The 2007 field experiment was designed to test the feasibility of proteomic sampling and analysis during acetate biostimulation of Fe(III)- and U(VI)-reducers, without initiating significant sulfate reduction. We analyzed data from the 2002 field experiment using characterized flow and transport properties from the previous modeling study (Yabusaki et al. 2007), determined field-scale reaction parameters for the modeled biogeochemical processes, then applied the calibrated process models directly to the 2003 and 2007 field experiments to compare with observations.

Calibrated Results for the 2002 Field Experiment**.** The calibration of the multicomponent biogeochemical reactive transport model for the 2002 biostimulation field experiment required a systematic approach to estimate both abiotic and biotic reaction parameters. In general, the simulated TEAP behaviors for Fe(III), U(VI), and sulfate were very similar to the Yabusaki et al. (2007) results. The abiotic reactions provided new insights on the pH and U(VI) surface complexation behavior (**Figure 5**) as well as the favorability of forming calcite and siderite.

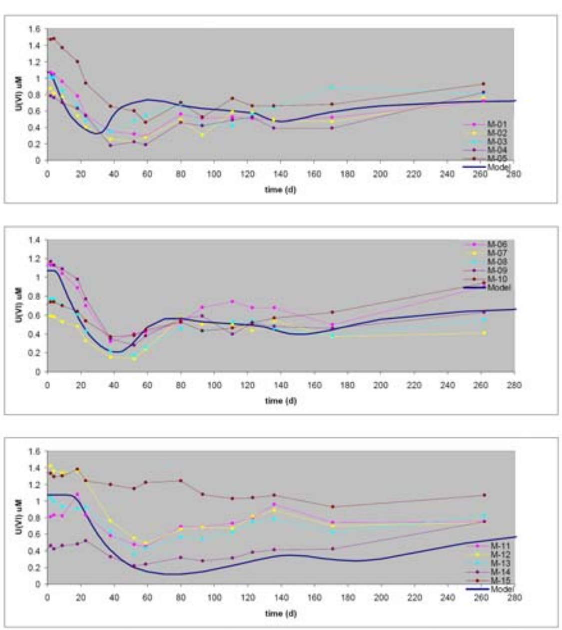

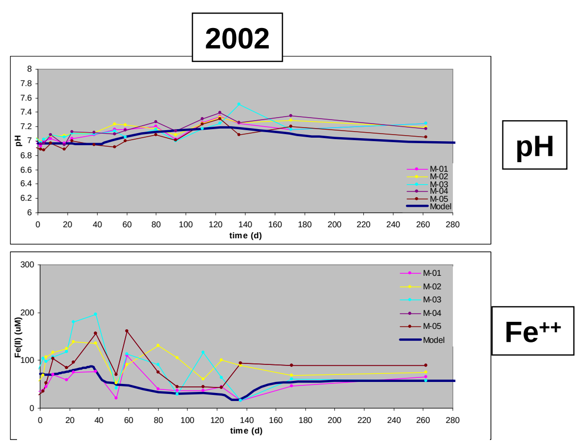

Figure 5. Observed (colored symbols/lines) and modeled (solid blue line) U(VI) (3.7 m, 7.3 m, and 14.6 m downgradient), pH (top) and dissolved Fe^{2+} (bottom) arriving at the monitoring wells 3.66 m downgradient from the injection gallery during the 2002 field experiment

Initially, acetate-oxidizing iron-reducers used silicate Fe(III), Fe-oxide and U(VI) as terminal electron acceptors resulting in an increase of Fe(II) and a decrease of U(VI) in solution. The onset of sulfate reduction occurred after a threshold amount of bioavailable phyllosilicate Fe(III) was consumed, resulting in lower sulfate concentrations. In the model, bioreduction is driven by the acetate amendment and stops when the acetate is no longer available. Consequently, there is a rebound in simulated sulfate and U(VI) concentrations after 136 days, when amendment is completely consumed or transported out of the system. During sulfate reduction, significantly more carbonate is generated which complexes with uranium to enhance uranium desorption from the sediment (**Figure 6**). The rate of uranium desorption from the sediment during sulfate reduction is faster than the bioconversion of U(VI) in the groundwater to U(IV) mineral. Once acetate injection is stopped, carbonate decreases to background concentrations resulting in stronger adsorption of uranium to the sediment and a long retarded rebound in uranium concentrations.

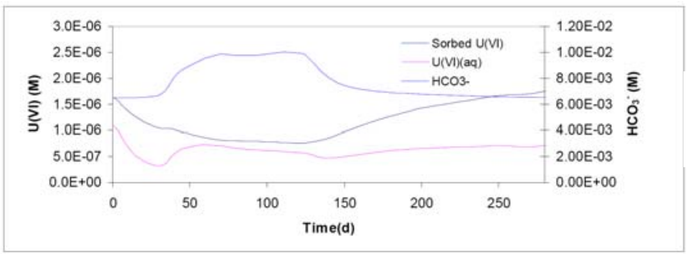

Figure 6. 2002 field experiment: simulated sorbed and aqueous U(VI), and bicarbonate 3.7 m downgradient from injection gallery.

The general trend of Fe(II) in solution was captured by the model: aqueous Fe(II) increases during iron reduction and decreases during sulfate reduction. During sulfate reduction, nearly 2 mM of sulfate is consumed while producing an equal amount of sulfide. However, very little aqueous sulfide is observed in the groundwater, which is consistent with the precipitation of amorphous FeS mineral. In the model, the sulfide is consumed by reacting with magnetite as other sediment-associated and biogenic Fe(II) sources are insufficient to completely react the generated sulfide. pH is generally buffered during iron reduction by the surface protonation and deprotonation reactions. During sulfate reduction, pH increases slightly by 0.2 log units because the magnetite reaction with HS^- results in a net consumption of protons. After the injection stops, pH gradually returns to the background condition. Simulated pH agrees well with the observations, which is very important for the pH-dependent uranium surface complexation behavior. Although calcite and siderite were predicted to precipitate during the 2002 biostimulation experiment, quantities were sufficiently small to have negligible impact on the pH, Fe(II) and U(VI) distributions.

It should be noted that the measured acetate and sulfate at downgradient monitoring wells are principally the result of reaction processes taking place in the first few meters beyond the injection gallery. After 52 days of simulation, there is a zone of depleted bioavailable Fe(III) mineral that is predicted to extend 7.5 meters from the injection gallery. While this zone defines where sulfate reducers can be active, the kinetics of the bioreduction result in 95% consumption of the acetate within 2.5 meters of the injection gallery. Consequently, the low acetate and sulfate concentrations observed in the downgradient monitoring wells reflect the transport rather than the local biogeochemistry of acetate and sulfate. Furthermore, the complete consumption of acetate would inactivate all modeled TEAPs in downgradient zones. This has significant implications for designing cost-effective bioremediation schemes to maintain the efficiency of uranium bioreduction. On the other hand, if the sulfate concentrations were relatively small, excess acetate would be available for continued reduction of U(VI) by iron reducers with access to bioavailable Fe(III).

Simulation of 2003 and 2007 Field Experiments. To test the consistency of the field-scale response during acetate biostimulation and the robustness of the biogeochemical reactive transport model, calibrated reaction parameters developed from the 2002 field experiment were applied without modification to the simulation of the 2003 and 2007 field biostimulation experiments.

In contrast to the 2002 experiment, which was performed in a subsurface system that had never experienced an acetate injection, the 2003 experiment began in the same previously biostimulated plot, albeit significantly depleted in “bioavailable” Fe(III) mineral. Furthermore, the acetate concentrations in the 2003 biostimulation were three times those used in the 2002 biostimulation. Simulation of the 2003 field experiment started from the conditions at the end of the simulation for the 2002 field experiment; i.e., simultaneous bioreduction of iron, uranium and sulfate. Fe(II) dynamics caused by the interplay of iron reduction, FeS precipitation and magnetite dissolution by sulfide, was simulated well by the model. In general, the simulated biogeochemical response to the biostimulation is quite consistent with the timing and magnitude of the field measurements (**Figure 7**).

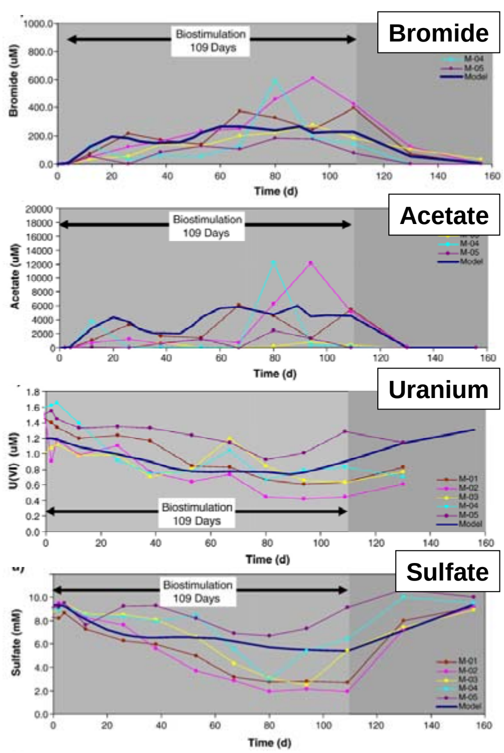

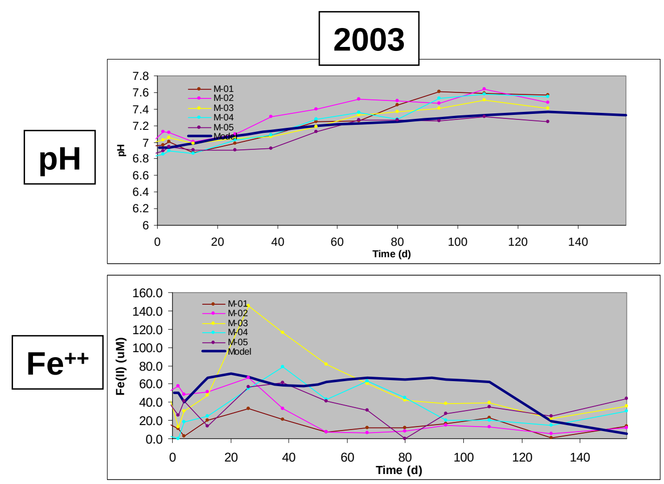

Figure 7. 2003 field experiment: simulated (dark blue line) and observed (colored lines/symbols) bromide, acetate, U(VI), sulfate, pH, and Fe^{2+} breakthrough 3.7 m downgradient from injection gallery.

The 2007 biostimulation field experiment was performed in a new location at the Rifle IFC site, approximately 35 m east-southeast of the 2002/2003 field plot. Based on the bromide tracer behavior during the 2007 field experiment, the 1-D hydrologic system was characterized by a Darcy flux of 0.055 m/d, a porosity of 0.15, and a dispersivity of 0.67

m. Reactions and rate parameters calibrated for the 2002 field experiment were then applied without modification to the 2007 experiment as well. In this case, an *in situ* concentration of 5 mM acetate (intermediate between the 2002 and 2003 field experiments) was targeted through the use of 10 injection wells employing a cross-well mixing scheme. To test the response of the microbial community to the dynamics of electron donor availability, biostimulation was stopped for 7 days after 11 days of acetate injection, then resumed for 12 more days. The relatively short biostimulation duration was designed to engineer iron and uranium bioreduction for proteogenomic sampling without transitioning to sulfate reducing conditions.

In general, the trend and magnitude of acetate, Fe(II), U(VI), sulfate, and pH behavior was captured by the multicomponent reactive transport simulation (**Figures 8 and 9**). Despite designing this experiment to stay in iron reduction, the model and the field data are consistent in showing the onset of sulfate reduction near the end of the biostimulation after 25 days. In the simulation, the rebound of uranium during sulfate reduction is caused by increasing carbonate complexation with uranium and lower uranium bioreduction in the system.

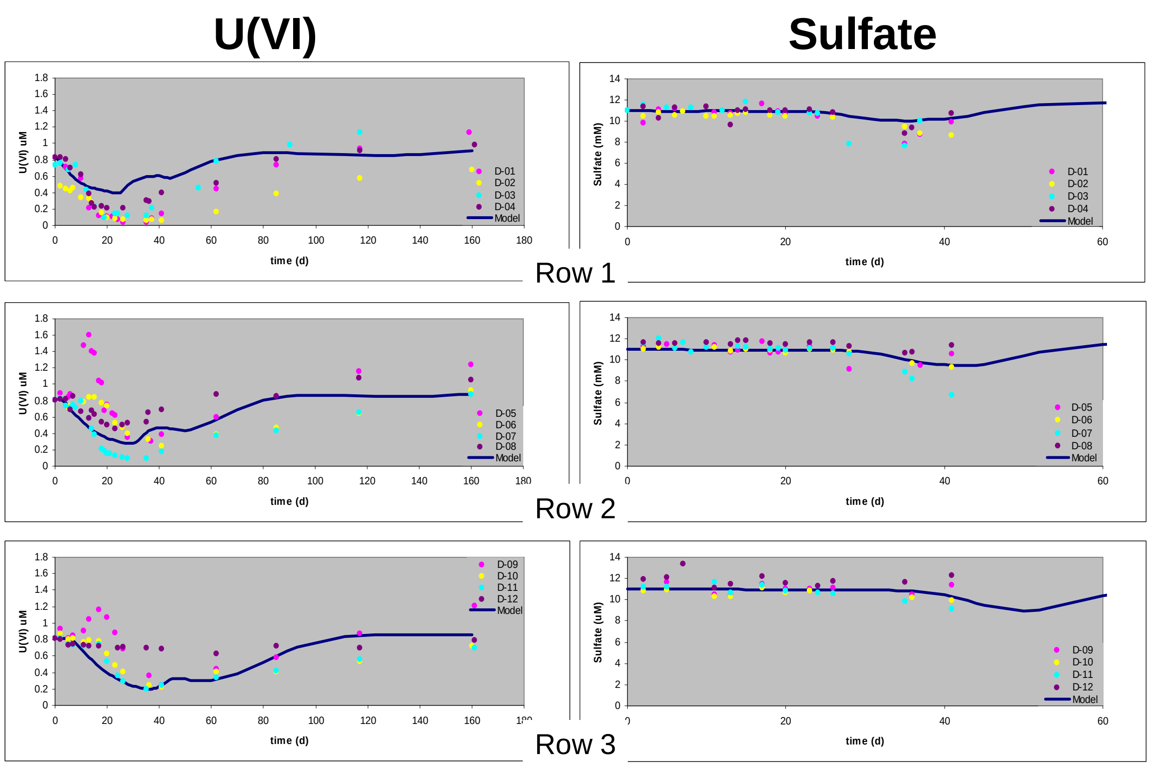

Figure 8. 2007 field experiment: simulated (dark blue line) and observed (colored symbols) U(VI) and sulfate concentrations 3.7 m downgradient from injection gallery.

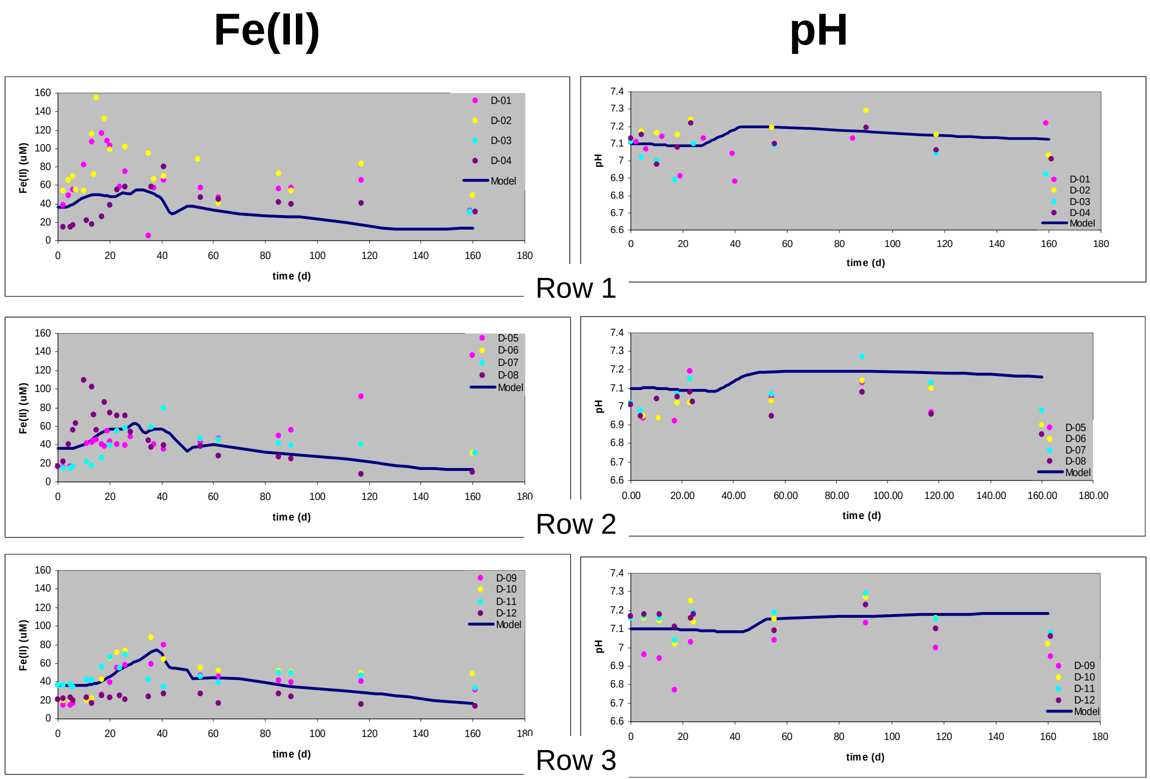

Figure 9. 2007 field experiment: simulated (dark blue line) and observed (colored symbols) Fe(II) concentrations and pH 3.7 m downgradient from injection gallery.

Summary

The multicomponent biogeochemical reactive transport model, calibrated with data from the 2002 field experiment at the Rifle IFC site, accounts for key terminal electron accepting processes and abiotic reaction processes in the 2003 and 2007 biostimulation field experiments. Despite different experimental locations and conditions, and variability in the timing and magnitude of the field behaviors, the model generally captures the observed dynamics in pH, U(VI), Fe(II), sulfate, and acetate. While we continue to refine the conceptual hydrologic, biological, and geochemical process models for the Rifle IFC site, the consistency of the current assumptions with the three large scale experiments implies a repeatable uranium bioremediation behavior that will be necessary for reliable engineering design.

For all three field experiments, the amounts of reduced phyllosilicate and oxide iron at the end of the simulations were consistent with laboratory studies, suggesting that the rate formulation is reasonable. Prior to the finding by Komlos et al. (2008) that the bulk of bioreduced iron was from phyllosilicate Fe(III), a more complicated modeling approach was needed to sorb Fe(II) liberated during the reductive dissolution of Fe(III) oxides. The large capacitance required for Fe(II) sorption resulted in a heavily damped Fe(II) behavior that was not sufficiently responsive to capture the observed magnitude and dynamics. In contrast, the immobile nature of the bioreduced phyllosilicate iron significantly minimizes the importance of including iron sorption, allowing for a decrease in the number of parameters to be calibrated while providing a better match to the observed behavior.

Another finding from the simulation is that enhanced production of carbonate during sulfate reduction may result in uranium desorption. At the end of the biostimulation when acetate was no longer available for the sulfate reducers, uranium sorption increased because the speciation favored uranium forms with higher affinity for the sediments. This might explain, in part, the post-biostimulation removal of uranium just after acetate amendment is discontinued.

Open Issues and Next Steps. The principal discrepancy between the simulated and observed uranium behavior occurs for the 2003 field experiment where there was a prolonged ca. 1.5 year post-biostimulation suppression of uranium concentrations in groundwater. In the current conceptual model, uranium sorption would be the only post-biostimulation process capable of continued removal of influent uranium. However, this would be considerably beyond the relatively short-term impact of potentially enhanced sorption processes. Furthermore, inclusion of uranium surface complexation during the biostimulation results in desorption of uranium that has not been observed in the laboratory (Ortiz-Bernad et al. 2004). The removal of U(VI) from groundwater long after cessation of electron donor amendment may depend on microbial communities that succeed iron reducers and sulfate reducers and may be linked to the occurrence of significant sulfate reduction during electron donor amendment (N'Guessan et al. 2008). This is the subject of ongoing study in the Rifle IFC project.

The current modeling approach has been able to reproduce the observed behavior of metal and sulfate reducing populations under the assumption of an attached microbial community. Yet, recent studies (Holmes et al. 2007) during in situ uranium bioremediation indicate that metabolically active *Geobacter s*pecies are highly planktonic in the subsurface during Fe(III) oxide bioreduction (Holmes et al., 2007). The necessity of incorporating this complexity remains an open issue. In addition, more detailed examination of the onset of sulfate reduction and its effect on sorption due to increased carbonate in the system is needed. In the 2007 experiment, acetate was turned off just as sulfate reduction was beginning, thus the effect of rapidly decreased bioreduction of U(VI) and the continuing influx of upgradient U(VI) into the experimental plot needs to be carefully compared to the onset of sulfate reduction.

Many of the modeled processes are inferred from a "weight of evidence" rather than direct verification. These processes include assumptions that 1) uranium is reduced only by the acetate-oxidizing dissimilatory metal reducing bacteria (i.e., *Geobacteraceae*), 2) the onset of sulfate reduction is triggered by the consumption of a threshold amount of Fe(III) mineral, and 3) the metal and sulfate reducing bacteria can be co-located and simultaneously active in the system. As our ability to assess the *in situ* metabolic status of individual populations rapidly improves, we expect in the near future to be able to verify or refute some of these assumptions. Key advancements allowing direct indication of specific metabolic activity include gene expression, proteogenomic analysis, stable isotope probing, and phospholipid fatty acid profiling. Coupling microbial function and activity with concomitant changes in chemical components at the site will allow us to build robust, quantitative linkages to the stoichiometry of biologically mediated reactions and associated rate laws in the context of the site-specific hydrological and geochemical system. In particular, cellularly mechanistic *in silico* models are being developed in coordination with the Rifle IFC project to describe the growth, metabolism, and function of the dominant microbial populations before, during, and after electron donor amendment. The goal is to integrate these quantitative, mechanistic microbial process models into the comprehensive, subsurface flow and biogeochemical reactive transport simulation capability.

This study underscores the importance of integrating abiotic chemistry with the microbially-mediated TEAPs in the reaction network to provide additional geochemical constraints for a more systematic and mechanistic interpretation of the field behaviors during biostimulation. The simulation framework constructed will also accommodate model refinement as new processes or mechanisms are identified.

References Cited

Anderson, R. T., H. A. Vrionis, I. Ortiz-Bernad, C. T. Resch, P. E. Long, R. Dayvault, K. Karp, S. Marutzky, D. R. Metzler, A. Peacock, D. C. White, M. Lowe and D. R. Lovley (2003). "Stimulating the in situ activity of Geobacter species to remove uranium from the groundwater of a uranium-contaminated aquifer." Applied and Environmental Microbiology **69**(10): 5884-5891.

Brooks, S. C., J. K. Fredrickson, S. L. Carroll, D. W. Kennedy, J. M. Zachara, A. E. Plymale, S. D. Kelly, K. M. Kemner and S. Fendorf (2003). "Inhibition of bacterial U(VI) reduction by calcium." Environmental Science & Technology **37**(9): 1850-1858.

Chang, Y. J., P. E. Long, R. Geyer, A. D. Peacock, C. T. Resch, K. Sublette, S. Pfiffner, A. Smithgall, R. T. Anderson, H. A. Vrionis, J. R. Stephen, R. Dayvault, I. Ortiz-Bernad, D. R. Lovley and D. C. White (2005). "Microbial incorporation of C-13-labeled acetate at the field scale: Detection of microbes responsible for reduction of U(VI)." Environmental Science & Technology **39**(23): 9039-9048.

Davis, J. A., D. E. Meece, M. Kohler and G. P. Curtis (2004). "Approaches to surface complexation modeling of uranium(VI) adsorption on aquifer sediments." Geochimica Et Cosmochimica Acta **68**(18): 3621-3641.

DOE (1999). Final site observational work plan for the UMTRA project Old Rifle site GJO-99-88-TAR. Grand Junction, Colo.

Doherty, J. (2004). PEST—Model-independent parameter estimation user's manual. 5th ed. Brisbane, Australia, Watermark Numerical Computing.

EPA (1998). U.S. Environmental Protection Agency Soil Cleanup Criteria in 40 CFR Part 192.

Fang, Y. L., S. B. Yabusaki and G. T. Yeh (2006). "A general simulator for reaction-based biogeochemical processes." Computers & Geosciences **32**(1): 64-72.

Fang, Y. L., G. T. Yeh and W. D. Burgos (2003). "A general paradigm to model reaction-based biogeochemical processes in batch systems." Water Resources Research **39**(4): -.

Finneran, K. T., R. T. Anderson, K. P. Nevin and D. R. Lovley (2002). "Potential for Bioremediation of uranium-contaminated aquifers with microbial U(VI) reduction." Soil & Sediment Contamination **11**(3): 339-357.

Gorby, Y. A. and D. R. Lovley (1992). "Enzymatic Uranium Precipitation." Environmental Science & Technology **26**(1): 205-207.

Holmes, D. E., K. T. Finneran, R. A. O'Neil and D. R. Lovley (2002). "Enrichment of members of the family Geobacteraceae associated with stimulation of dissimilatory metal reduction in uranium-contaminated aquifer sediments." Applied and Environmental Microbiology **68**(5): 2300-2306.

Holmes, D. E., R. A. O'Neil, H. A. Vrionis, L. A. N'Guessan, I. Ortiz-Bernad, M. J. Larrahondo, L. A. Adams, J. A. Ward, J. S. Nicoll, K. P. Nevin, M. A. Chavan, J. P. Johnson, P. E. Long and D. R. Lovley (2007). "Subsurface clade of Geobacteraceae that predominates in a diversity of Fe(III)-reducing subsurface environments." Isme Journal **1**(8): 663-677.

Hunter, K. S., Y. F. Wang and P. Van Cappellen (1998). "Kinetic modeling of microbially-driven redox chemistry of subsurface environments: coupling transport, microbial metabolism and geochemistry." Journal of Hydrology **209**(1-4): 53-80.

Kindred, J. S. and M. A. Celia (1989). "Contaminant Transport and Biodegradation .2. Conceptual-Model and Test Simulations." Water Resources Research **25**(6): 1149-1159.

Kinzelbach, W., W. Schafer and J. Herzer (1991). "Numerical Modeling of Natural and Enhanced Denitrification Processes in Aquifers." Water Resources Research **27**(6): 1123-1135.

Komlos, J., A. Peacock, R. K. Kukkadapu and P. R. Jaffe (2008). "Long-Term Dynamics of Uranium Reduction/Reoxidation under Low Sulfate Conditions." Geochimica Et Cosmochimica Acta **In Press**.

Lovley, D. R., E. J. P. Phillips, Y. A. Gorby and E. R. Landa (1991). "Microbial Reduction of Uranium." Nature **350**(6317): 413-416.

Lovley, D. R., E. E. Roden, E. J. P. Phillips and J. C. Woodward (1993). "Enzymatic Iron and Uranium Reduction by Sulfate-Reducing Bacteria." Marine Geology **113**(1-2): 41-53.

Moon, H. S., J. Komlos and P. R. Jaffe (2007). "Uranium reoxidation in previously bioreduced sediment by dissolved oxygen and nitrate." Environmental Science & Technology **41**(13): 4587-4592.

Moyes, L. N., R. H. Parkman, J. M. Charnock, D. J. Vaughan, F. R. Livens, C. R. Hughes and A. Braithwaite (2000). "Uranium uptake from aqueous solution by interaction with goethite, lepidocrocite, muscovite, and mackinawite: An X-ray absorption spectroscopy study." Environmental Science & Technology **34**(6): 1062-1068.

N'Guessan, A. L., H. A. Vrionis, C. T. Resch, P. E. Long and D. R. Lovley (2008). "Sustained Removal of Uranium From Contaminated Groundwater Following Stimulation of Dissimilatory Metal Reduction." Environmental Science & Technology **42**(8): 2999-3004.

Ortiz-Bernad, I., R. T. Anderson, H. A. Vrionis and D. R. Lovley (2004). "Resistance of solid-phase U(VI) to microbial reduction during in situ bioremediation of uranium-contaminated groundwater." Applied and Environmental Microbiology **70**(12): 7558-7560.

Pabalan, R. T., F. P. Bertetti, J. D. Prikryl and D. R. Turner (1996). "Uranium(VI) sorption onto selected mineral surfaces: Key geochemical parameters." Abstracts of Papers of the American Chemical Society **211**: 55-Geoc.

Park, S. S. and P. R. Jaffe (1996). "Development of a sediment redox potential model for the assessment of postdepositional metal mobility." Ecological Modelling **91**(1-3): 169-181.

Rabouille, C. and J. F. Gaillard (1991). "A Coupled Model Representing the Deep-Sea Organic-Carbon Mineralization and Oxygen-Consumption in Surficial Sediments." Journal of Geophysical Research-Oceans **96**(C2): 2761-2776.

Rittmann, B. E. and P. L. McCarty (2001). Environmental biotechnology : principles and applications. Boston, McGraw-Hill.

Vrionis, H. A., R. T. Anderson, I. Ortiz-Bernad, K. R. O'Neill, C. T. Resch, A. D. Peacock, R. Dayvault, D. C. White, P. E. Long and D. R. Lovley (2005). "Microbiological and geochemical heterogeneity in an in situ uranium bioremediation field site." Applied and Environmental Microbiology **71**(10): 6308-6318.

Wolery, T. J. (1992). EQ3/6, A Software Package for Geochemical Modeling of Aqueous Systems. Version 7.0, Lawrence Livermore National Laboratory/University of. Livermore, California.

Yabusaki, S. B., Y. Fang, P. E. Long, C. T. Resch, A. D. Peacock, J. Komlos, P. R. Jaffe, S. J. Morrison, R. D. Dayvault, D. C. White and R. T. Anderson (2007). "Uranium Removal from Groundwater via In Situ Biostimulation: Field-Scale Modeling of Transport and Biological Processes." Journal of Contaminant Hydrology **93**(1-4): 216-235.

Yeh, G. T., Y. Li, P. M. Jardine, W. D. Burgos, Y. Fang, M.-H. Li and W. D. Siegel (2004). HYDROGEOCHEM 4.0: A coupled model of fluid flow, thermal transport, and HYDROGEOCHEMical transport through saturated-unsaturated media: version 4.0. . Oak Ridge, Tennessee, Oak Ridge National Laboratory.